

## Flame propagation in random media

N. Provatas,<sup>1</sup> T. Ala-Nissila,<sup>1,2,3</sup> Martin Grant,<sup>1</sup> K. R. Elder,<sup>1</sup> and Luc Piché<sup>1,4</sup>

<sup>1</sup>*McGill University, Physics Department and Centre for the Physics of Materials, 3600 rue University, Montréal, Québec, Canada H3A 2T8*

<sup>2</sup>*Research Institute for Theoretical Physics, University of Helsinki,*

*P.O. Box 9 (Siltavuorenpenger 20 C), FIN-00014 University of Helsinki, Finland*

<sup>3</sup>*Brown University, Department of Physics, Box 1843, Providence, Rhode Island 02912*

<sup>4</sup>*National Research Council, Industrial Materials Institute, 75 De Mortagne Boulevard, Boucherville, Québec, Canada J4B 6Y4*

(Received 26 April 1994)

We introduce a phase-field model to describe the dynamics of a self-sustaining propagating combustion front within a medium of randomly distributed reactants. Numerical simulations of this model show that a flame front exists for reactant concentration  $c > c^* > 0$ , while its vanishing at  $c^*$  is consistent with mean-field percolation theory. For  $c > c^*$ , we find that the interface associated with the diffuse combustion zone exhibits kinetic roughening characteristic of the Kardar-Parisi-Zhang equation.

PACS number(s): 05.70.Ln, 64.60.Ht, 68.35.Fx, 05.40.+j

The behavior of a nonequilibrium system is often limited by a reaction front between one metastable or unstable phase and another more stable phase. A common but spectacular example of this occurs in slow combustion where a flame front forms and can propagate [1–6]. Here we study a phase field model of combustion in the absence of convection and apply methods developed in the study of phase transitions to the asymptotic behavior of a self-sustaining combustion front growing within a medium of randomly distributed reactants. Both the formation of the front as well as its universal dependence on length and time are examined. We find numerically that the combustion front exists for reactant concentration  $c > c^* > 0$  in  $d = 2$  dimensions, where the behavior at  $c^*$  is consistent with that of mean-field percolation. For  $c > c^*$ , we find that the diffuse combustion zone exhibits kinetic roughening characteristic of the Kardar-Parisi-Zhang interface equation [7].

While we expect our phase-field model to describe the universal features of combustion or reaction fronts in the absence of convection, we shall motivate it below in terms of a specific example, forest fires. The physics associated with forest fires has recently received attention [2–4] due to the potential relationship with the concept of self-organized criticality, introduced by Bak [5] and collaborators. In most cases studied to date, cellular automaton models on a lattice have been used [2–4]. In these works a collection of forests which can burn and subsequently reappear is considered. In contrast, this paper focuses on systems in which the reacting element cannot spontaneously reappear. It is worth noting that although our paper is partly motivated by this work, we shall not directly address issues such as self-organized criticality.

Our model consists of two coupled reaction-diffusion equations, one governing the concentration of reactants, and the other the dynamics of a thermal field. Unlike discrete lattice models, this model incorporates the in-

terplay between long-range thermal diffusion and local random concentration fields. Within our model, variations in the local temperature field  $T(\vec{x}, t)$  at position  $\vec{x}$  and time  $t$  are due to three effects: (i) thermal diffusion through the medium; (ii) Newtonian cooling due to coupling to a heat bath; and (iii) generation of heat, limited by activation, from the reactants. Explicitly, the temperature field obeys

$$\frac{\partial T}{\partial t} = D\nabla^2 T - \Gamma[T - T_0] - \vec{V} \cdot \vec{\nabla} T + R(T, C), \quad (1)$$

where  $D$  is the diffusion coefficient,  $\Gamma$  is the thermal dissipation constant, and  $T_0$  is the constant background temperature of the bath responsible for Newtonian cooling. For completeness we have included convection due to an external forcing  $\vec{V}$ , but we shall hereafter set this term to zero.

Nonlinearities enter through the reaction rate  $R(T, C)$ , which is limited by a field  $C$  describing the local concentration of reactants. Activation implies that this term is proportional to  $\exp(-A/T)$ , where  $A$  is an activation energy, and Boltzmann's constant has been set to unity. Furthermore the rate is limited by the local flux  $\propto \sqrt{T}$ , so that the local energy produced per unit time is proportional to  $q(T) = T^{3/2} \exp(-A/T)$ , where the additional factor of  $T$  sets the scale of energy. In the combustion literature [1], the multiplicative prefactor is  $T^\alpha$ , where  $\alpha = O(1)$  varies according to the conditions present. However, the particular form is relatively unimportant since the dominating temperature dependence is the exponential activation. Hence, on measuring temperature in units of the activation energy, we model the reaction rate as

$$R = \lambda_2 \left( T^{3/2} e^{-1/T} \right) C = -\lambda_1 \frac{\partial C}{\partial t}, \quad (2)$$

where  $\lambda_1$  is a dimensionless constant. This completes the

formulation. Initial conditions on the field  $C$  determine the random distribution and concentration of reactant. Here we have initially distributed the reactant at random, with the probability that a given system site is occupied being  $c$ , where the field variable  $C$  equals 1 on an occupied site and zero if the site is unoccupied.

For the remainder of this paper, we consider  $d = 2$ , where a front initially parallel to the  $y$  axis propagates in the  $x$  direction. The dimensionless parameters are set to  $D = 0.2$ ,  $\Gamma = 0.05$ ,  $T_0 = 0.01$ , and  $\lambda_1 = 8$ , time is measured in units of those for the reaction  $\lambda_2/\lambda_1$ , and length in units of the dimension of the reactant. In our numerical work, the mesh size in space is set to  $\Delta x = 1$ , while the mesh size in time is  $\Delta t = 0.01$ ; tests of smaller mesh sizes give qualitatively similar results. It is useful to relate these choices of parameters to the specific example of a forest fire. For example, the constant  $\lambda_2$  in Eq. (2) can be found in terms of the density and specific heat of air and the activation temperature of wood [10]. In physical units, we have  $D \sim 1 \text{ m}^2 \text{ s}^{-1}$ ,  $\Gamma \sim 0.05 \text{ s}^{-1}$ ,  $T_0 \sim 10 \text{ K}$ ,  $c_p \sim 5 \text{ J g}^{-1} \text{ K}^{-1}$ , and  $A \sim 500 \text{ K}$ . With the exception of  $T_0$ , these are comparable to real systems. Our small  $T_0$  has been chosen to give enhanced cooling and hence keep diffusion fields relatively short ranged. This allows us to perform our numerical integrations with good accuracy without having to simulate extremely large systems. Test runs show that our results are relatively insensitive to the choice of  $T_0$ .

Due to the activated nature of the combustion process, a self-sustaining propagating combustion front requires a sufficient amount of heat to be released during combustion. The source for this heat is the reactant concentration  $c$ . Since activation limits the production of this heat, we expect existence of a nonzero concentration  $c^*$ , below which the fire will spontaneously burn out due to insufficient heat production. That is, for  $c < c^*$  the velocity of the front  $v(c) = 0$ , while  $v$  is nonzero for higher concentrations. For quantitative analysis the position  $h(y, t)$  of the front, where  $v = \partial h / \partial t$ , is defined as the position  $x$  where the temperature is maximum at a given time and  $y$  position. The variable  $h$  is then a single-valued function of  $y$ .

For large concentrations,  $v$  is constant after an initial transient, and increases with  $c$ . The transient increases as  $c^*$  is approached. In the vicinity of  $c^*$ , the asymptotic velocity approaches the relationship  $v(c) \sim (c - c^*)^\phi$ , where  $\phi$  is an exponent similar to that obtained in percolation theory [9].

To determine the scaling exponent in the case of a random background, Eqs. (2) and (3) were numerically solved on a lattice using periodic boundary conditions in the  $y$  direction and fixed boundary conditions in the  $x$  direction. The dimension of the system is  $L$  in the  $y$  direction, and well exceeds  $vt_{\text{max}}$  in the  $x$  direction, where  $t_{\text{max}}$  is the maximum time studied. At every site, the concentration variable  $C$  is initially either zero or 1, and randomly distributed with average  $c$ . The fire is started at the far left by igniting a complete row of "trees" at  $y = 0$ . After a short transient, the propagating fire front assumes a steady-state average velocity  $v(c)$ . In Figs. 1(a) and 1(b) typical configurations of the

propagating temperature field are shown at  $c = 0.65$  and  $0.225$ . For lower densities, the front becomes very irregular and finally stops propagating. Calculating the velocity numerically for  $L = 200$  we find  $c^* = 0.19 \pm 0.02$  and  $\phi = 0.46 \pm 0.09$ .

Mean-field theory is useful to understand these percolation results. Consider a uniform distribution of reactants, whose density variable  $C$  is everywhere equal to  $c$ . In this description there are no longer variations in  $T$  in the  $y$  direction. Assume there exists a mean-field temperature front  $T_m$  moving with constant velocity  $v_m(c)$ . Using  $\partial T / \partial t = -v_m dT / dx$ , we obtain a nonlinear consistency relation between  $T_m$  and  $v_m(c)$ . We have solved this mean field model numerically, revealing a dependence of  $v_m(c)$  in  $c$  of the form  $v_m(c) \propto (c - c^*)^\phi$ , near  $c^* = 0.19$ , where  $\phi = 0.5$ . The exponent  $\phi = 1/2$  is also a consequence of the following argument. Let  $x_t$  be a point sufficiently ahead of the peak of  $T_m$ , beyond which dissipation exceeds activation in the thermal diffusion equation. Expanding  $R(T)$  to linear order around  $T_{\text{tail}} \equiv T_m(x_t)$ , we find that the leading edge of  $T_m$  goes as  $T_m \sim \exp(\{-v_m - \sqrt{v_m^2 - 4D[\lambda_1 C_{\text{tail}} q'(T_{\text{tail}}) - \Gamma] / 2D}x\})$ , where  $C_{\text{tail}} \equiv C(x_t)$ . The requirement that  $T_m$  does not develop any oscillatory components gives, for  $c$  near  $c^*$ ,  $v_m \geq A(c - c^*)^{1/2}$ , with  $c$  implicitly defined by  $c^* = \Gamma / [q'(T_{\text{tail}}^*) \lambda_1]$ , and where  $T_{\text{tail}}^*$  implies evaluation at  $c = c^*$ . This analysis is analogous to the method used in Ref. [11] to find front velocities in the context of epidemic models, and we expect that near  $c = c^*$ ,  $v_m$  will approach its lower bound.

To incorporate finite-size effects, we use a scaling form

$$v(c, L) \sim L^{-\phi/\nu} \Omega[(c - c^*)L^{1/\nu}]. \quad (3)$$

This is the same as that used in percolation theory [8]. Here  $\nu$  is the correlation-length exponent  $\xi \sim (c - c^*)^{-\nu}$ , and the scaling function  $\Omega(x \rightarrow \infty) \sim x^\phi$ . We relate  $\phi$  to the percolation transition exponents through  $v(c) \sim \xi/\tau \sim (c - c^*)^{\Delta - \nu}$ , where  $\Delta$  is the critical slowing down exponent, so that  $\phi = \Delta - \nu$ . In Fig. 2, we show numerical results for  $v(c, L)L^{\phi/\nu}$  vs  $(c - c^*)L^{1/\nu}$  for nine different system sizes ranging from  $L = 4$  to  $L = 200$ . Using  $c^* = 0.19$  and  $\phi = 0.46$ , we find that the best collapse occurs for  $\nu = 0.6 \pm 0.1$ , as shown in Fig. 2.

The results for the critical exponents are consistent with the mean-field exponents of percolation, for which  $\phi = \nu = \Delta/2 = 1/2$  [9]. Qualitatively, heat propagation in our model is limited by a percolation lattice, provided by the random density field  $C$ . Below  $c^*$ , the connected cluster available for front propagation breaks down, and the fire spontaneously dies out. The mean-field nature of the critical exponents is due to the extended nature of the diffusion field associated with  $T$ . We see no numerical evidence for a crossover to non-mean-field exponents for the realistic parameters we have used.

For  $c > c^*$ , it is clear from Fig. 1 that the propagating interface associated with  $T$  develops large fluctuations and appears rough. We define the width of the interface by  $w = \langle (h - \langle h \rangle)^2 \rangle^{1/2}$ . Rough interfaces often satisfy the scaling relation [7,12]  $w(t, L) \sim t^\beta f(t/L^z)$  for large

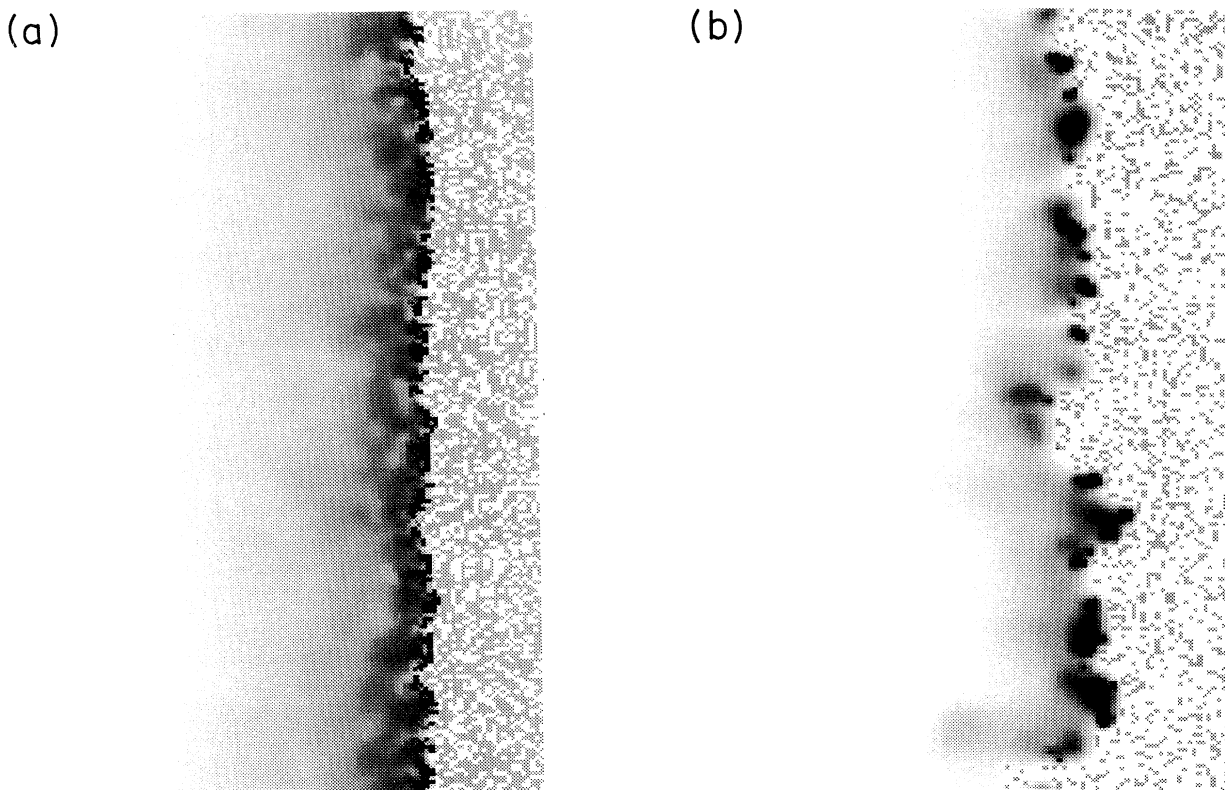


FIG. 1. The temperature field  $T(x, y, t)$  for a moving fire front in a uniform, random forest with (a)  $c = 0.65$  and (b)  $c = 0.225$ . The dark pixels correspond to the temperature field; the higher the temperature the darker the pixels. The interface  $h(y, t)$  is defined by the curve outlined by the darkest pixels. The light grey pixels to the right of the interface represent reactant.

$L$  and  $t$ . An important example of this is the Kardar-Parisi-Zhang (KPZ) interface equation [7], for which the exact and nontrivial exponents are  $\beta = 1/3$ ,  $z = 3/2$ , and  $\chi = z\beta = 1/2$ , in  $d = 2$ . In our case, for any given value of  $c > c^*$ , we expect the width to obey this scaling form, i.e., for large  $t$ , we expect  $w \sim t^\beta$  in the limit  $t \ll L^z$ , where finite-size effects can be neglected. To account for the dependence of the width on concentration in this limit, we propose

$$w(c, t) = \xi(c)w_s[t/\tau(c)], \quad (4)$$

where  $w_s(t \rightarrow \infty) \sim t^\beta$ , and for  $c$  near  $c^*$ ,  $\xi(c) \sim (c - c^*)^{-\nu}$  and  $\tau(c) \sim (c - c^*)^{-\Delta}$ . It is straightforward to generalize this form to include finite-size effects. In Fig. 3 we show the scaled width  $w_s$  plotted vs the scaled time  $t_s = t/\tau$ , for seven different values of  $c$  with  $L = 200$ . For this  $L$ , finite-size effects play no discernible role. The inset shows the original data set. A transient time  $t_0$  has been subtracted, which has been determined from the point where  $v(c)$  reaches a constant value. From the fitted  $\xi(c)$  and  $\tau(c)$  for the data collapse we cannot accurately estimate  $\nu$  and  $\Delta$ , although they are consistent with the mean-field values.

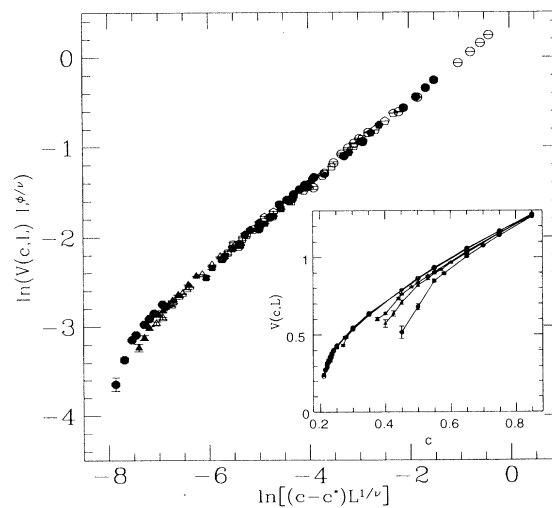


FIG. 2. Finite size scaling of  $v(c, L)$ . The main figure shows  $\ln(v(c, L)L^{\phi/\nu})$  vs  $\ln((c - c^*)L^{1/\nu})$ . The inset shows the unscaled data for system sizes  $L = 4, 6, 8, 24, 44, 54, 64, 104,$  and  $200$ , from right to left. Sizes larger than  $L = 24$  lie almost on the same curve.

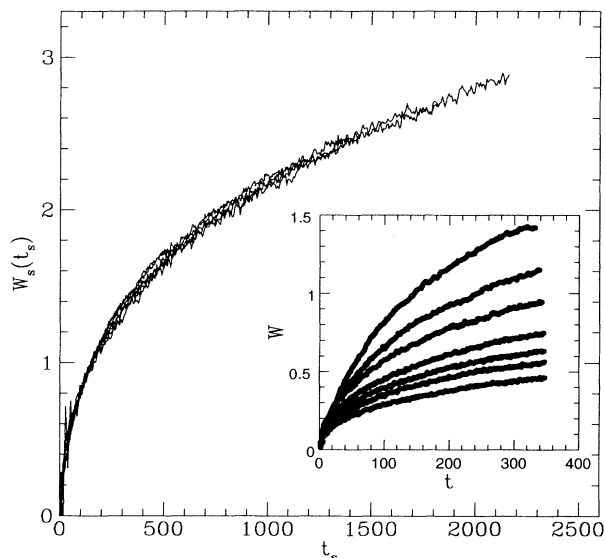


FIG. 3. Crossover scaling function  $w_s$  plotted vs  $t_s = t/\tau$ . The inset shows the concentration dependent width  $w(c, t)$ , for  $c = 0.4, 0.5, 0.6, 0.7, 0.75, 0.80$ , and  $0.85$  from top to bottom. The roughness increases with decreasing density. A transient time  $t_0$  and the corresponding offset  $w_0$  have been subtracted from each  $w(c, t)$

From the scaled data of Fig. 3, we determine the roughening exponent  $\beta$ . The running slope of the data from a  $\ln w$  vs  $\ln t$  plot gives an effective  $\beta(t)$ , which is shown in Fig. 4. After an initial transient the slope clearly tends towards  $\beta = 1/3$ , which is the exact KPZ value. We have also analyzed the data by calculating the difference  $w(bt) - w(t) = A(b^\beta - 1)t^\beta$ , where  $b$  is a constant (e.g.,  $b = 2$ ). From this we find  $\beta = 0.34 \pm 0.04$ , which is our best estimate of this exponent.

In the limit where the width saturates due to finite-size effects, i.e.,  $t \gg L^z$ , the scaling relation gives  $w(c, L) \sim L^\chi$ . Using system sizes  $L = 50, 76, 100, 150, 200, 300, 400$ , and  $600$ , we obtain  $\chi = 0.5 \pm 0.1$  for  $c = 0.5$  and  $\chi = 0.5 \pm 0.2$  for  $c = 0.85$ , as compared to the exact KPZ value of  $\chi = 1/2$ . Our results for  $\beta$  and  $\chi$  are therefore in good agreement with those of the KPZ equation [7,6].

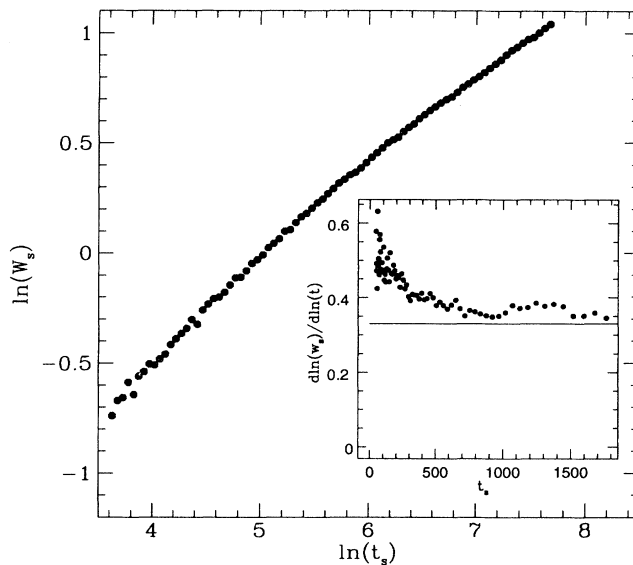


FIG. 4. A log-log plot of the scaling function  $w_s$  of Fig. 3. The inset shows the effective  $\beta$  as a function of time. The straight line represents  $\beta = 1/3$ .

To summarize, in this work we have developed a realistic phase-field model for combustion fronts. We find a percolation transition at a critical reactant density  $c^* \approx 0.19$ , below which the fire will spontaneously die. We have analyzed the nature of this transition and found critical exponents which are consistent with those of mean-field percolation. Furthermore, above  $c^*$ , we found that the diffuse combustion front displays kinetic roughening. By an appropriate generalization of the usual scaling form for interfaces, we have shown that the roughening exponents are compatible with the KPZ universality class.

The Centre for Scientific Computing (CSC) Co. of Espoo, Finland has provided most of the computing resources for this work. This work has also been supported by the Academy of Finland, the Natural Sciences and Engineering research Council of Canada, and les Fonds pour la Formation de Chercheurs et l'Aide à la Recherche de Québec.

- [1] F. A. Williams, *Combustion Theory*, 2nd ed. (Benjamin Cummings Publishing Company, New York, 1985).
- [2] G. Albinet, G. Searby, and D. Stauffer, *J. Phys.* **47**, 1 (1986).
- [3] P. Bak, K. Chen, and C. Tang, *Phys. Lett. A* **147**, 297 (1990).
- [4] B. Drossel and F. Schwabl, *Phys. Rev. Lett.* **69**, 1629 (1992); P. Grassberger and H. Kantz, *J. Stat. Phys.* **63**, 685 (1991).
- [5] P. Bak, C. Tang, and K. Wiesenfeld, *Phys. Rev. Lett.* **59**, 381 (1987).
- [6] Recently, J. Zhang, Y. C. Zhang, P. Alström, and M. T. Levinsen [*Physica A* **189**, 383 (1992)] have interpreted the results of burning sheets of paper in terms of kinetic

- roughening. They found  $\chi \sim 0.71$ , which is larger than we find. This may be due to the correlated distribution of fibers within paper.
- [7] M. Kardar, G. Parisi, and Y. C. Zhang, *Phys. Rev. Lett.* **56**, 889 (1986); for a review see J. Krug and H. Spohn, in *Solids Far from Equilibrium: Growth, Morphology, and Defects*, edited by G. Godreche (Cambridge University Press, Cambridge, 1991).
- [8] D. Stauffer, *Introduction to Percolation Theory*, 2nd ed. (Taylor & Francis, London, 1985).
- [9] D. Stauffer, *Phys. Rep.* **54**, 3 (1979).
- [10] For a rough estimate of the parameters entering our model for the specific case of a forest fire, we assume trees burn via a steady-state reaction with air, treating air as

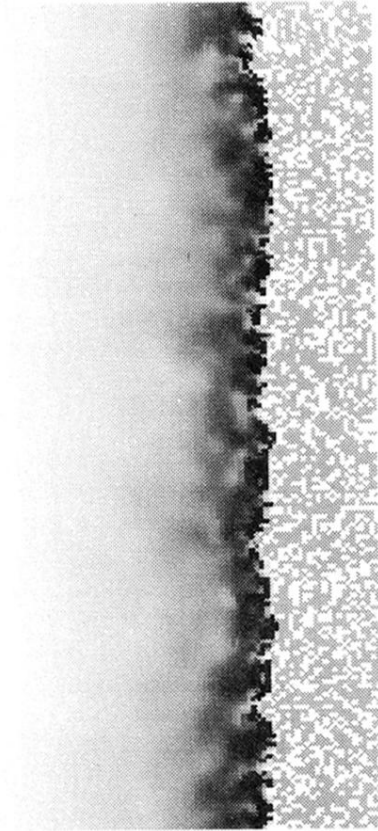
an ideal gas. The flux of molecules striking the wood surface is  $N_s = (n/4)\sqrt{(2T/m)}$ , where  $n$  is the number density and  $m$  is the mass per molecule in air. Since the number of molecules reacting is  $N_r = N_s e^{-A/T}$ , the energy  $Q$  released per unit tree area and time equals the energy of the molecules entering the reaction,  $Q = (3T/2)N_s e^{A/T}$ . If  $r$  is a tree radius, the heat given off per unit volume of a tree site and per unit time is  $2Q/r$ . Writing  $T$  in units of

$A$ , the temperature change per unit time corresponding to this heat production is  $(2Q/r)/(c_p \rho)$ , where  $c_p$  is the specific heat and  $\rho$  is the mass density of air. Now, on recalling that we are scaling temperature in units of  $A$ , we obtain the parameter  $\lambda_2 = (3\sqrt{2}/4rc_p)(1/m)^{3/2}(A)^{1/2}$ .

[11] J. D. Murray, *Mathematical Biology* (Springer Verlag, Berlin, 1989).

[12] F. Family and T. Vicsek, *J. Phys. A* **18**, L57 (1985).

(a)



(b)

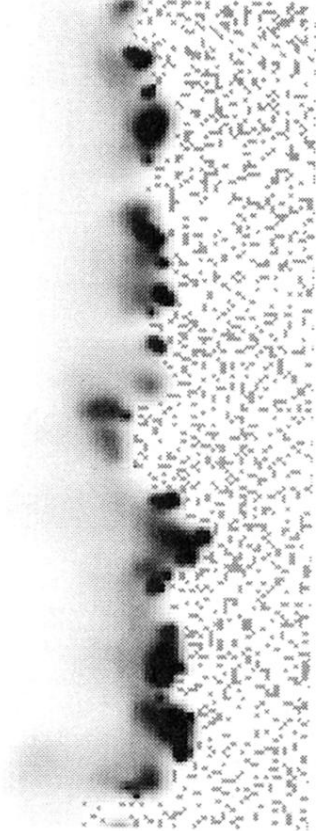


FIG. 1. The temperature field  $T(x, y, t)$  for a moving fire front in a uniform, random forest with (a)  $c = 0.65$  and (b)  $c = 0.225$ . The dark pixels correspond to the temperature field; the higher the temperature the darker the pixels. The interface  $h(y, t)$  is defined by the curve outlined by the darkest pixels. The light grey pixels to the right of the interface represent reactant.